The Journal of Experimental Biology 211, 341-353
Published by The Company of Biologists 2008
doi:10.1242/jeb.012682

Performance trade-offs in the flight initiation of *Drosophila*

Gwyneth Card* and Michael Dickinson
Bioengineering, California Institute of Technology, Pasadena, CA 91125, USA
*Author for correspondence (e-mail: gwyneth@caltech.edu)

Accepted 12 November 2007

SUMMARY

The fruit fly *Drosophila melanogaster* performs at least two distinct types of flight initiation. One kind is a stereotyped escape response to a visual stimulus that is mediated by the hard-wired giant fiber neural pathway, and the other is a more variable 'voluntary' response that can be performed without giant fiber activation. Because the simpler escape take-offs are apparently successful, it is unclear why the fly has multiple pathways to coordinate flight initiation. In this study we use high-speed videography to observe flight initiation in unrestrained wild-type flies and assess the flight performance of each of the two types of take-off. Three-dimensional kinematic analysis of take-off sequences indicates that wing use during the jumping phase of flight initiation is essential for stabilizing flight. During voluntary take-offs, early wing elevation leads to a slower and more stable take-off. In contrast, during visually elicited escapes, the wings are pulled down close to the body during take-off, resulting in tumbling flights in which the fly translates faster but also rotates rapidly about all three of its body axes. Additionally, we find evidence that the power delivered by the legs is substantially greater during visually elicited escapes than during voluntary take-offs. Thus, we find that the two types of *Drosophila* flight initiation result in different flight performances once the fly is airborne, and that these performances are distinguished by a trade-off between speed and stability.

Supplementary material available online at http://jeb.biologists.org/cgi/content/full/211/3/341/DC1

Key words: *Drosophila*, escape response, giant fiber.

INTRODUCTION

The flight initiation behavior of *Drosophila melanogaster* is an attractive model system for the study of sensory-motor integration, as it is a tractable system in which different sensory modalities are believed to trigger different descending pathways to elicit a take-off. During a spontaneous take-off, or when stimulated by an attractive odor, a fly first raises its wings to a ready position that it may hold for several seconds. It then extends its mesothoracic legs while depressing its wings, thus coordinating a jump with the initial downstroke (Trimarchi and Schneiderman, 1995a; Hammond and O'Shea, 2007b). In contrast, strong visual stimuli, such as a rapid drop in luminance, cause a fly to quickly extend its middle legs, propelling itself off the ground in less than 5 ms without the aid of coordinated wing motion. This simpler visually elicited escape response is mediated by the well-characterized giant fiber (GF) interneurons (for a review, see Allen et al., 2006), whereas spontaneous or odor-induced take-offs are thought to involve a separate descending pathway (Holmqvist, 1994; Trimarchi and Schneiderman, 1995b; Trimarchi and Schneiderman, 1995c).

The GFs are a pair of large interneurons that traverse the cervical connective, linking sensory regions of the fly's brain to motor centers in its thoracoabdominal ganglion. In the thorax, each giant fiber contacts the ipsilateral motorneuron of the fly's main jump muscle (the tergotrochanteral muscle, TTM) and the peripherally synapsing interneuron (PSI), which crosses the midline to innervate the motorneurons of all six indirect wing depressors (dorsal longitudinal muscles, DLMs) (Allen et al., 2006). When contracted, the TTMs extend the femur of the fly's mesothoracic legs. Thus it is this middle pair of legs that provides the main leg force during both voluntary and escape jumps (Nachtigall and Wilson, 1967; Tanouye and Wyman, 1980). The GFs in *Drosophila* are thought to receive input primarily from visual areas of the brain (Kaplan and Trout, 1974; Levine, 1974; Thomas and Wyman, 1984; Holmqvist and Srinivasan, 1991), and it was demonstrated directly that a light-off stimulus activates the giant fiber in white-eyed *Drosophila* mutants (Trimarchi and Schneiderman, 1995a). However, in larger flies, such as the house fly *Musca domestica*, it has been shown that the GFs also receive mechanosensory input from the antennae, and possibly ascending input from the tarsal mechanoreceptors (Bacon and Strausfeld, 1986).

Activation of the GFs, either directly *via* a stimulating electrode or by a light-off stimulus, results in a stereotyped pattern of muscle potentials with characteristic latencies. As implied by the anatomy, giant fiber stimulation first elicits a TTM muscle spike, followed by activation of the DLMs (Tanouye and Wyman, 1980). Recently, Lima and Miesenbock coupled expression of the ligand-gated $P2X_2$ ion channel with injections of an optically caged agonist to drive GF activation in intact animals using pulses of light (Lima and Miesenbock, 2005). Freely moving animals initiated flight when the giant fibers were activated with light pulses, confirming that these neurons are sufficient to elicit an escape response.

Although the function of the GF pathway in the escape response seems clear, the anatomy and functional role of the other pathways that can initiate flight are not. Several lines of evidence suggest that both odor-induced and spontaneous take-offs proceed without activation of the GFs, observations that argue for the existence of a separate descending pathway (Holmqvist, 1994; Trimarchi and Schneiderman, 1995b; Trimarchi and Schneiderman, 1995c). There is even evidence that the GFs are neither the only, nor even the first, descending pathway activated during visually elicited escape responses: contrary to previous observations, a recent study using high-speed imaging found that *Drosophila* begin to raise their

wings before they start to jump in response to a looming visual stimulus (Hammond and O'Shea, 2007a). Because the GF pathway is not known to activate any wing-elevator muscles prior to the jump muscle, Hammond and O'Shea suggested that a non-GF descending pathway that coordinates wing-raising may be activated before the GF in response to a looming threat.

If the anatomical arrangement of the GF pathway is sufficient to generate a take-off during escape responses, why are other pathways necessary to elicit other forms of flight initiation? A study using hummingbirds (Tobalske et al., 2004) found that different levels of motivation result in different take-off performance. Thus, one possibility is that various types of take-off behavior are optimized for different performance requirements, and that these are mediated by different neural circuits. In order to test this hypothesis, we used 3D high-speed video techniques to quantitatively analyze the body dynamics and performance of *Drosophila* during take-offs initiated under different stimulus conditions. Our results suggest that different flight initiation circuits may have evolved to selectively emphasize either launch velocity or stability, two incompatible features of take-off performance.

MATERIALS AND METHODS

Animals

In all experiments we used 3-day old mated female *Drosophila melanogaster* (Meigen) taken from the lab colony, which is descended from 200 wild-caught females. Flies were reared in incubators at 25°C, and tested at room temperature (22–25°C).

High-speed videography

Three high-speed video cameras (Photron Ultima APX, San Diego, CA, USA) captured freely moving flies taking off in orthogonal views. Take-offs were filmed at 6000 frames s^{-1} with 512×512 pixel resolution, using 50 mm Nikon lenses (Nikon USA, Melville, NY, USA) with (1:2) extension tubes to obtain the desired magnification. We calibrated the cameras using the Direct Linear Transform method (Abdel-Aziz and Karara, 1971). A single LED, mounted on a micromanipulator and moved to known positions in the filming volume, served as the calibration object.

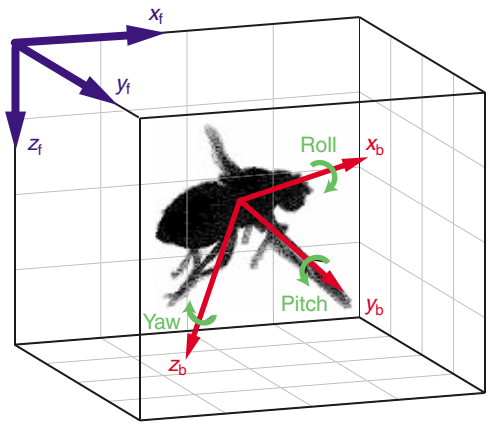

Fig. 1. Definition of kinematic frames of reference. The fixed lab frame (x_f, y_f, z_f) is a right-handed coordinate system with the positive z_f-axis pointing down towards the ground. A second frame of reference (x_b, y_b, z_b) has its origin at the fly's center of mass with the x_b-axis oriented along the long body axis towards the animal's head, the y_b-axis oriented parallel to the fly's right wing, and the z_b-axis positioned perpendicular to the x_b- and y_b-axes and directed towards the ventral surface of the animal. Right-wing down rotation about the x_b-axis is positive roll, nose-up rotation around the y_b-axis is positive pitch, and a turn to the fly's right around the z_b-axis is positive yaw. For each video frame, a unit quaternion $\boldsymbol{q}$ specifies the rotation from body-centered coordinates to the fixed lab coordinates necessary to achieve the attitude of the fly in that frame.

To correctly position a fly in the focal planes of all three cameras simultaneously, we focused each camera on the tip of a glass pipette fixed at an angle of approximately 45° from the horizontal. We introduced individual flies into the bottom of the pipette, and the animals crawled upward by positive geotaxis until they emerged at the tip, maximizing the probability that the fly was in focus in all three views at the start of the take-off.

Voluntary take-offs

Upon emerging from the pipette tip, most flies chose to stand or groom themselves. At this point we began capturing images with the cameras set in a continuous capture mode. Those flies that walked off the pipette were not used. Flies were permitted to remain on the pipette undisturbed until they flew away. For convenience, we will term these un-elicited take-offs as 'voluntary' although we do not presume any complex cognitive processing by the fly's brain. We recorded voluntary take-offs by manually post-triggering the camera to save all frames captured 1.7 s prior to the trigger point. Voluntary take-offs occurred anywhere from 1 to 60 min after the fly climbed to the top of the pipette. In some cases, the flies were deprived of water for several hours before the experiment to increase the frequency of voluntary take-offs.

Escape responses

We triggered escape behaviors with a physical black disk falling on a collision course with the fly. The disk consisted of a 140 mm-diameter foam board circle covered with black felt. A small hole in the center of the disk allowed it to slide 190 mm down a plastic rod angled 50° from the horizontal. The falling disk subtended a visual angle of 20° at its starting point and 40° at its final point in the fly's field of view. The disk thus provided a very strong looming stimulus to the fly, similar to the visual stimulation that might be created by a predator or approaching fly swatter. We have previously reported preliminary results indicating that this stimulus is effective for eliciting escapes in wild type *Drosophila* (Card et al., 2005). We started the falling disk manually by pulling on a long rod that acted as a block to keep the disk from descending. We triggered the disk within several seconds of the fly emerging onto the platform, but only after the fly had settled down into a stationary position. As the disk fell, it passed a photodiode/detector pair, which generated an electrical pulse that served as the recording trigger. A plastic stopper prevented the disk from sliding off the end of the rod. The disk did bounce slightly when it hit the stopper, but in all experiments the escaping flies had left the substratum before the disk reached the end of the rod. We determined the time course of the falling disk by filming it with the high-speed video cameras and digitizing its position along the rod.

Clipped-wing flies

To assess the role played by the wings during escape take-offs, we filmed flies with their wings removed taking off in response to the falling disk. In these clipped-wing trials, we anesthetized individual flies by cooling them to 4°C using a Peltier system and then excised both wings at the wing hinge. We then isolated each fly in a small vial and left them to recover for at least 30 min before introducing them into the high-speed video apparatus. In order to capture the entire escape jump trajectory we used a slower recording rate

(2000 frames s^{-1}) and lower camera lens magnification to film clipped-wing trials.

Analysis

To compare the coordinated action of wings and legs in the observed types of take-off, we recorded the timing of wing and leg events from each video sequence. Most event timings were not normally distributed within each stimulus condition (Lillie test for normality, $P<0.025$), so we use non-parametric statistics to report our findings: the median (med) is the middle value in our observed data range, and the interquartile range (IQR) is the range around the median including 50% of the data.

To assess differences in body kinematics and flight performance between the two different types of take-off, we digitized the long (abdomen to head) and transverse (left to right wing hinge) axes of the fly in each of the three orthogonally arranged cameras. Position data were smoothed using a zero-phase-lag 4th order Butterworth filter (cut-off frequency 250 Hz, or 60 Hz for clipped-wing flies). As a rough guess, we estimated the center of mass (COM) of the fly as the point along the long body axis 50% of the distance from the head to the end of the abdomen. COM calculations made from a 3D model of a fruit fly body and from 2D video images (assuming uniform density) confirmed that this is a reasonable estimate. COM velocities and accelerations were determined by fitting the smoothed position data with a cubic spline and taking the first and second derivatives of the spline without further smoothing (equivalent to applying the Central Difference Theorem).

Following the convention from aerodynamics described by Phillips (Phillips, 2004), we defined two frames of reference to describe the kinematic data: the fixed lab frame (x_f, y_f, z_f) and the animal's body-centered frame (x_b, y_b, z_b). In this scheme, rotations around the body-centered x_b, y_b and z_b axes are called roll, pitch and yaw, respectively (Fig. 1). Note that these body angles are distinct from an Euler angle system in which three successive rotations about non-orthogonal axes define the attitude of the rotated object. The three Euler rotation angles are sometimes also called roll, pitch and yaw (Schilistra and van Hateren, 1999), but in our convention they are referred to as bank, elevation and heading (see supplementary material Fig. S2). As Euler angle schemes are subject to singularities ('gimbal lock') when rotations are large, a more convenient way to express the three-dimensional rotation of a rigid body is with a quaternion. Quaternions are an extension of the complex number system for which a unit quaternion $\mathbf{q}$ can be thought of as representing a rotation of θ radians about a 3D axis defined by the vector $\mathbf{v}$ such that (Kuipers, 2002):

$$\mathbf{q} = \cos(\theta/2) + \mathbf{v}\sin(\theta/2) \, . \quad (1)$$

We determined roll, pitch and yaw velocities $\boldsymbol{\omega}$ by expressing the three-dimensional rotations about the COM as unit quaternions $\mathbf{q}$ and solving the equation:

$$d\mathbf{q}/dt = \tfrac{1}{2}\mathbf{q} \otimes \boldsymbol{\omega} \, , \quad (2)$$

where $\otimes$ indicates quaternion multiplication (Phillips, 2004). Angular position was then determined from the rotational velocities by a cumulative sum, and acceleration was calculated using the spline method described above. Because of the geometry of the glass pipette substrate from which the flies took off, some flies had initial 'roll' and 'pitch' angles relative to the lab coordinate frame. These starting angles were added to the rotational velocity cumulative sum so that initial roll and pitch position values are expressed in the context of the lab frame. Initial yaw orientations were also arbitrary, but have no systematic implications for flight control, and so for calculating mean time courses they are expressed relative to starting position (i.e. initial yaw is always 0°). All digitization and analysis was performed using custom programs written in Matlab (Mathworks, Natick, MA, USA). Most kinematic parameters were normally distributed within stimulus condition groups (Lillie test, $P>0.025$), so kinematic data are reported as mean ± s.e.m.

From the measured kinematic parameters, we can estimate the kinetic and potential energy of the fly during flight initiation. Translational kinetic energy KE_{trans} of a fly with mass m and translational speed v is:

$$KE_{trans} = 0.5mv^2 \, . \quad (3)$$

Rotational kinetic energy, KE_{rot}, can be calculated as the vector product:

$$KE_{rot} = 0.5\mathbf{I}\boldsymbol{\omega}^2 \, , \quad (4)$$

where $\mathbf{I}$ is the moment of inertia tensor for an ellipsoid body, and $\boldsymbol{\omega}$ is the angular velocity vector. The potential energy PE of the fly is calculated from the fly's height off the substrate, z, and the acceleration due to gravity $\boldsymbol{g}$, as:

$$PE = m\boldsymbol{g}z \, . \quad (5)$$

We estimate the average total energy of the fly during the first 2 ms after take-off as the sum of translational, rotational and potential energies during this period.

RESULTS

We analyzed 16 voluntary take-offs and 27 escape responses captured on videotape. Our analysis excluded 25 additional take-off sequences (4 voluntary, 21 escape) in which one or both of the fly's middle legs slipped on the pipette during leg extension.

Voluntary flight initiations

As previously described (Trimarchi and Schneiderman, 1995a), we observed that flight initiations performed in the absence of any overt stimulus consisted of at least two distinct phases: wing raising and subsequently leg extension. First, the fly elevated and then supinated its wings so that the ventral surface of each wing faced out laterally with the leading edge forward. Second, the mesothoracic legs extended at the coxotrochanteral, femorotibial and tibiotarsal joints. The motion of the legs and wings were coordinated so that at the start of leg extension the wings elevated further (first upstroke), but then quickly depressed downward (first downstroke) as the legs completed their extension (Fig. 2A). Fig. 3A shows the relative timing of wing and leg motion for all voluntary take-offs analyzed.

We found that the time between first wing-raising movements and the start of leg extension (41.7 ms, IQR=46.3, N=16, Fig. 3A) was substantially longer and more variable than previously reported (10.5±5.4 ms, mean ± s.d., N=4) (Trimarchi and Schneiderman, 1995a). We also observed that the timing of wing raising varies not only from event to event, but from wing to wing. In other words, the fly typically did not raise the left and right wing in unison. In only three of the 16 voluntary take-offs that we digitized did the wings begin to rise simultaneously within the resolution of our frame rate. This observation confirms a recent report (Hammond and O'Shea, 2007b). In our sample, 8/16 flies began flight initiation by raising the right wing first, whereas 5/16 flies began with the left. The first wing raised always corresponded with whichever wing happened to be on top at rest.

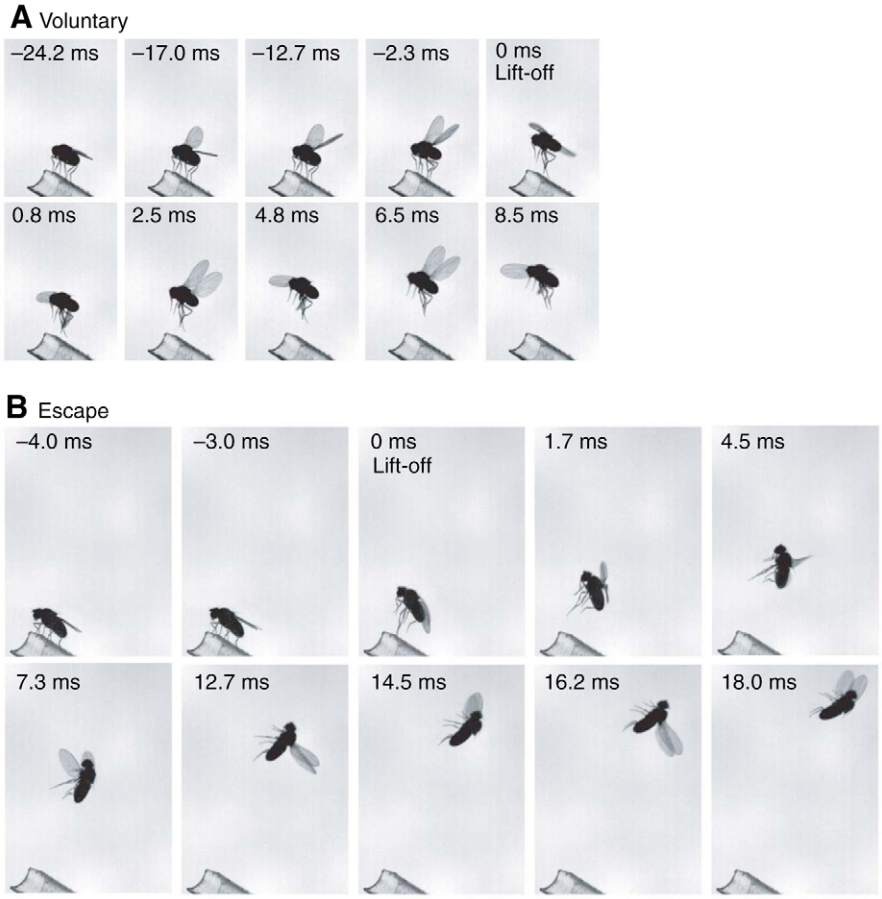

Fig. 2. Video sequences for (A) voluntary and (B) escape take-offs. Only one of the three camera views is shown. Times noted are ms from lift-off, the first frame in which both the fly's mesothoracic legs are no longer touching the substrate. For complete video sequences, see supplementary material Movies 1 and 2.

The median time lag between the start of top and bottom wing opening was 7.0 ms (IQR=17.7). The duration of wing opening (interval from start of motion until wing stops in fully raised position) was not significantly different between right and left wings (right: 10.7 ms, IQR=15.3; left: 11.5 ms, IQR=11.3; P=0.75, Kruskal–Wallis test).

Escape responses

In our experiments, 95% of the flies stimulated with the falling black disk took off between the moment the stimulus was released (t=0) and the time the stimulus reached the end of the rod (t=228 ms, Fig. 4). Flies that initiated flight outside this time window were not considered to have responded to the disk stimulus and were discarded. A sample video sequence of an escape take-off is shown in Fig. 2B, and timelines for all analyzed escape take-offs are shown in Fig. 3B.

From our data, it is clear that wing raising preceded leg extension in almost all (96%) escape responses. This agrees well with recent observations (Hammond and O'Shea, 2007a) in a similar preparation. In some cases, the wings were fully elevated prior to the jump and the overall pattern resembled a voluntary take-off. In 80% of the cases (22/27) in which wing motion preceded leg extension, however, one or both wings never reached full extension before the legs began to kick, at which point the wings were pulled back against the body. As a consequence, most escape jumps occurred with the wings in the closed position, as originally observed (Trimarchi and Schneiderman, 1995a), and the flies attempted to open their wings only after they were fully airborne (see supplementary material Fig. S1).

Opening the wings completely after the jump often took several wing strokes to accomplish. During the first few upstrokes, the wings bent substantially at a flexure point that was distal to the actual wing hinge (Fig. 5; also Fig. 2B, fourth panel). This bending pattern contrasted sharply with the normal flight pattern in which the wings move smoothly about the hinge with little flexure (Fry et al., 2005). Wings displayed this peculiar upstroke-bending pattern for 2–6 strokes until they were successfully unfurled during a downstroke. Left and right wings could unfurl independently. In some cases one wing would continue to bend on the upstroke even after the other wing was fully open and flapping normally (Fig. 3B).

For a subset of the escape responses (N=17), we also measured the timing of the escape response relative to the action of the falling black disk stimulus. The median escape take-off latency was 190.7 ms (IQR=15.3) from the start of stimulus motion, and flies began wing motion within a range of 160–210 ms from the start of the stimulus (Fig. 4). During this period, the disk diameter had reached a size of 30–40° in the fly's field of view. The rather large range in reaction times (~50 ms) could be related to the fact that the flies oriented themselves roughly randomly when they emerged at the pipette tip, so that in some cases the disk approached from the front, whereas in other cases it fell towards the back or side of the fly.

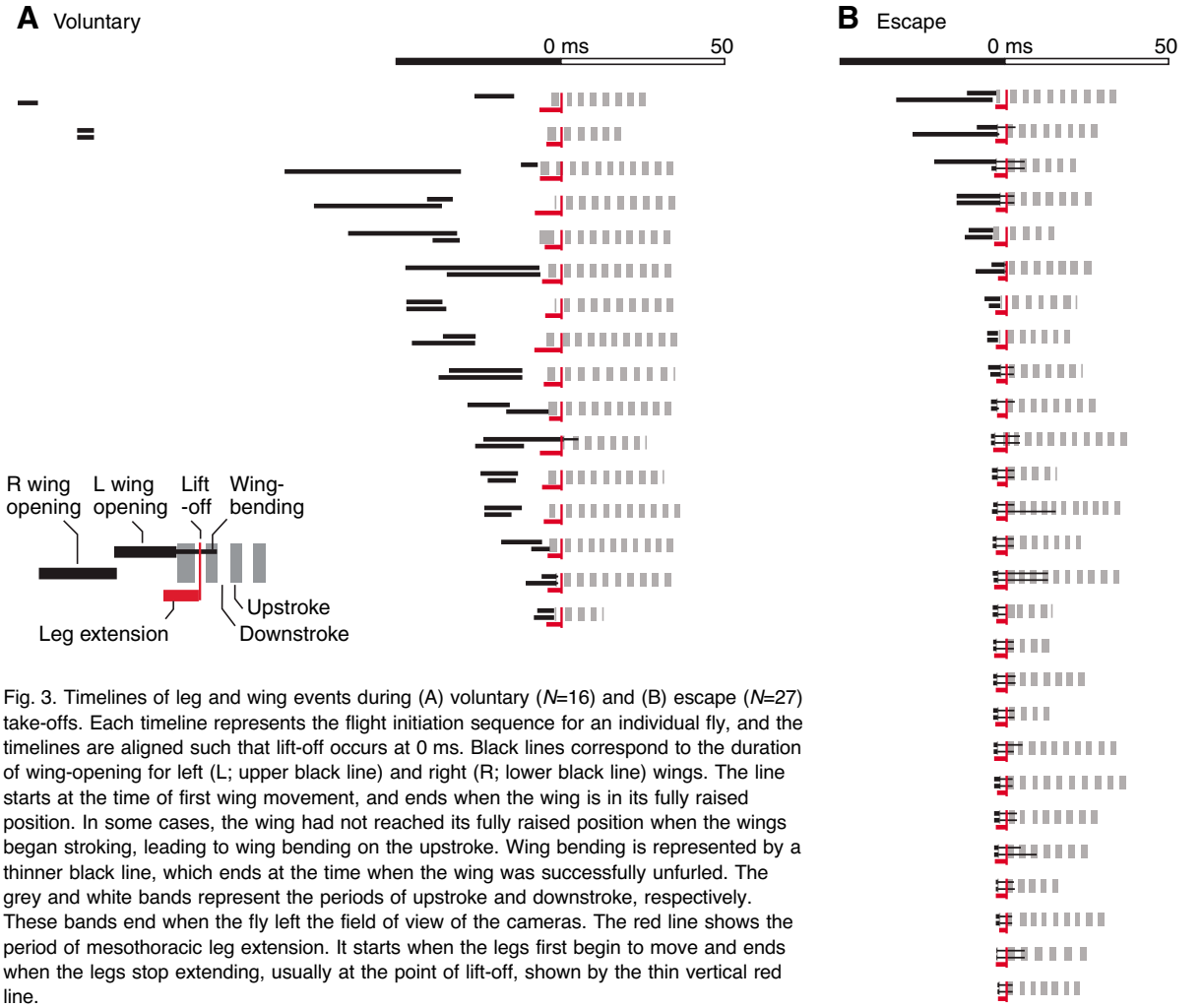

Fig. 3. Timelines of leg and wing events during (A) voluntary (*N*=16) and (B) escape (*N*=27) take-offs. Each timeline represents the flight initiation sequence for an individual fly, and the timelines are aligned such that lift-off occurs at 0 ms. Black lines correspond to the duration of wing-opening for left (L; upper black line) and right (R; lower black line) wings. The line starts at the time of first wing movement, and ends when the wing is in its fully raised position. In some cases, the wing had not reached its fully raised position when the wings began stroking, leading to wing bending on the upstroke. Wing bending is represented by a thinner black line, which ends at the time when the wing was successfully unfurled. The grey and white bands represent the periods of upstroke and downstroke, respectively. These bands end when the fly left the field of view of the cameras. The red line shows the period of mesothoracic leg extension. It starts when the legs first begin to move and ends when the legs stop extending, usually at the point of lift-off, shown by the thin vertical red line.

Comparison of escape and voluntary take-off behaviors

We found significant differences between voluntary and escape take-offs with respect to three temporal measures: wing–leg interval, leg-downstroke interval, and the period of leg extension (Table 1). The time between the start of wing opening and the onset of leg extension (wing–leg interval) was much longer and more variable for voluntary (34.83 ms, IQR=45.4) compared to escape take-offs (1.0 ms, IQR=2.7) (see also Hammond and O'Shea, 2007a). The time between the start of leg extension and the start of the first downstroke (leg-downstroke interval) was also longer and more variable for voluntary (3.3 ms, IQR=2.3) compared to escape take-offs (0.67 ms, IQR=0.83). This interval is of particular interest because a short latency between leg extensor and wing depressor muscle activation is a hallmark of the giant fiber pathway. In electrophysiological experiments, GF stimulation results in a short and fixed latency between TTM and DLM activation [0.44±0.05 ms delay (Tanouye and Wyman, 1980); 0.4–0.8 ms, (Trimarchi and Schneiderman, 1995c)]. Finally, voluntary take-offs exhibited a significantly longer period of leg extension compared to escapes (5.5 ms, IQR=2.0 *vs* 3.3 ms, IQR=0.46), similar to the difference recently reported (Hammond and O'Shea, 2007b).

Voluntary and escape take-offs also differed significantly in the stroke frequency of the first several wing beats once airborne. For the first three strokes, flies taking off voluntarily flapped at an average rate of 261 Hz (IQR=26.6) compared to 277 Hz (IQR=11.2) for escaping flies. These wing beat frequencies are 20–30% higher than the 200–220 Hz wing beat frequency measured for steadily hovering flies in free flight (Fry et al., 2005).

Table 1. Timing of voluntary and escape take-off events

Event	Median (IQR)		Significant difference	*P*-value*
	Voluntary	Escape		
Start of stimulus to lift-off (ms)	–	190.67 (15.29)	–	–
L–R wing interlatency (ms)	7.00 (17.67)	0.00 (0.58)	0	0.446
Left wing opening (ms)	11.50 (11.25)	–	–	–
Right wing opening (ms)	10.75 (15.25)	–	–	–
Wing–leg interval (ms)	34.83 (45.42)	1.00 (2.67)	1	<0.001
Leg-downstroke interval (ms)	3.33 (2.33)	0.67 (0.83)	1	<0.001
Leg extension (ms)	5.50 (2.00)	3.33 (0.46)	1	<0.001
Wing-beat frequency (Hz)†	261 (11.2)	277 (26.6)	1	0.001

*Kruskal–Wallis test.
†Average of first three strokes.

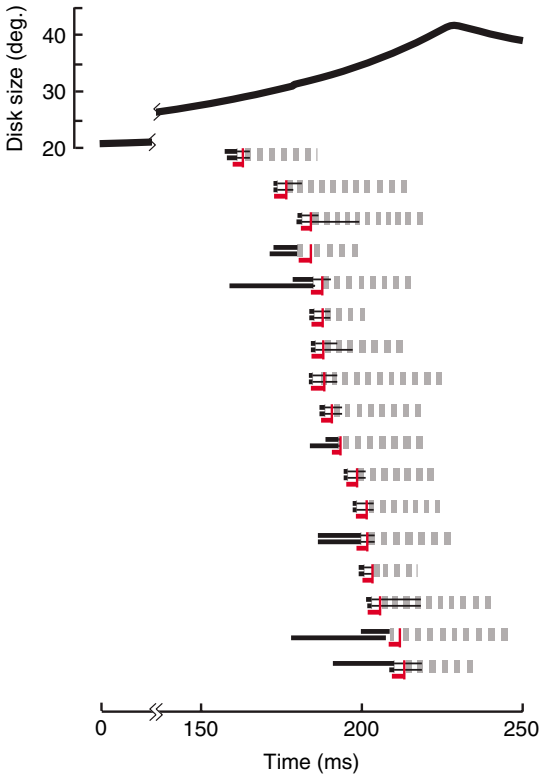

Fig. 4. Latency of escape take-offs. Timelines of the subset of escape responses for which latency was measured are plotted in relation to the angular size of the falling black disk stimulus in the fly's visual field. Timeline notation is as in Fig. 2 (*N*=17).

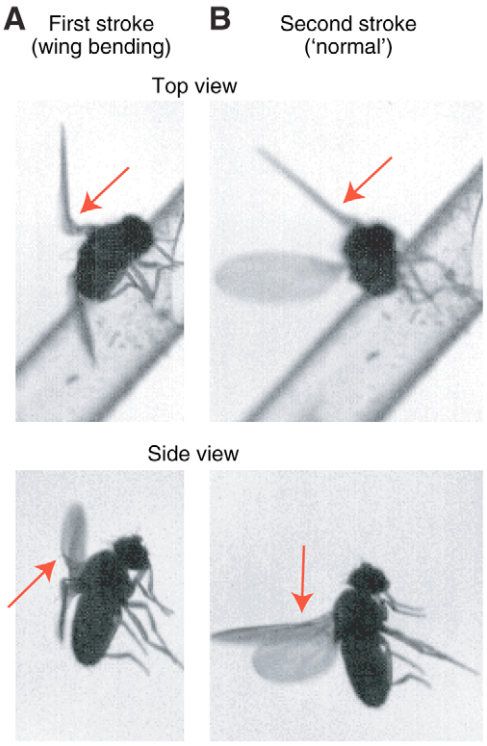

Fig. 5. Wing bending during the first upstroke. The images show a comparison of wing shape during the first upstroke after take-off (A) and the second upstroke (B) of an example escape take-off. Two camera views are shown for each stroke (top and side views). The images show the fly's wing position 7 frames (1.2 ms) after the start of the respective upstrokes. The red arrows point to a flexure point along the left wing. The wing bends nearly 90° at this point during the first upstroke, but only minimal bend is evident during the second, more 'normal' upstroke (see also supplementary material Movie 3). The right wing also appears to bend in a similar fashion.

Flight initiation kinematics

To assess flight performance during and after flight initiation, we recorded voluntary and escape take-offs in 3D using multiple camera views. Fig. 6 shows example trajectories for a voluntary take-off (Fig. 6A) and an escape response (Fig. 6B). In both examples, the fly's center of mass (COM) was stationary immediately before the jump as the wings elevated, accelerated during the leg-extension period, and continued with positive translational velocity once airborne. The escaping fly also underwent notable rotational velocities about all three axes and in the air.

Fig. 7 shows the mean (± s.e.m.) translational and rotational body kinematics for all 43 flies digitized. To enable pooling of results, we arbitrarily transformed each individual trajectory so that all first yawing and rolling motions were to the right. We did not transform the pitch angle in this way, because head-down pitch and head-up pitch have very different functional implications for flight. However, 39 out of 43 flies started take-off with a head-up pitching motion, an observation which suggests that the ground reaction forces generated by the mesothoracic legs during the jump are typically oriented anterior to the fly's center of mass.

On average, both the horizontal and vertical components of center of mass acceleration during escapes were nearly twice those during voluntary take-offs (Fig. 7A). Peak vertical acceleration was 57.0 m s^{-2} (IQR=35.8) for voluntary take-offs and 112 m s^{-2} (IQR=47.8) for escapes ($P \ll 0.001$, Kruskal–Wallis test). Peak horizontal acceleration was 46.1 m s^{-2} (IQR=28.8) and 107 m s^{-2} (IQR=50.0) for voluntary take-offs and escapes, respectively ($P \ll 0.001$, Kruskal–Wallis test). In both cases, the ratio of vertical to horizontal peak acceleration was close to 1, indicating the fly typically launched itself into the air with a take-off angle of roughly 45° from the horizontal. If the fly were purely ballistic, this is the expected launch angle to maximize horizontal distance traveled.

A plot of the mean time courses for angular accelerations during voluntary take-offs (Fig. 7B) show that both pitch and yaw accelerations reached a peak during leg extension but decayed quickly once the fly was airborne. In contrast, roll acceleration maintained a plateau for nearly 5 ms after lift-off, which suggests that the flies are generating roll actively with their wings. Mean peak velocities around all three axes were of similar magnitude, approximately 2000–3000 deg. s^{-1}. These values are comparable to maximum yaw velocity during saccade maneuvers in free-flying *Drosophila* (1800 deg. s^{-1}) (Fry et al., 2003) and maximum roll velocity during a variety of maneuvers in free-flying houseflies (3000 deg. s^{-1}) (Schilistra and van Hateren, 1999). On average, roll and yaw velocities decayed after the first 10 ms of flight, whereas pitch velocities did not decline to zero until after 20 ms from lift-off.

Escape take-offs produced substantially larger angular accelerations and higher rotational velocities around all three body axes compared to voluntary take-offs, and the differences were most striking in roll. Average peak pitch and yaw velocities were

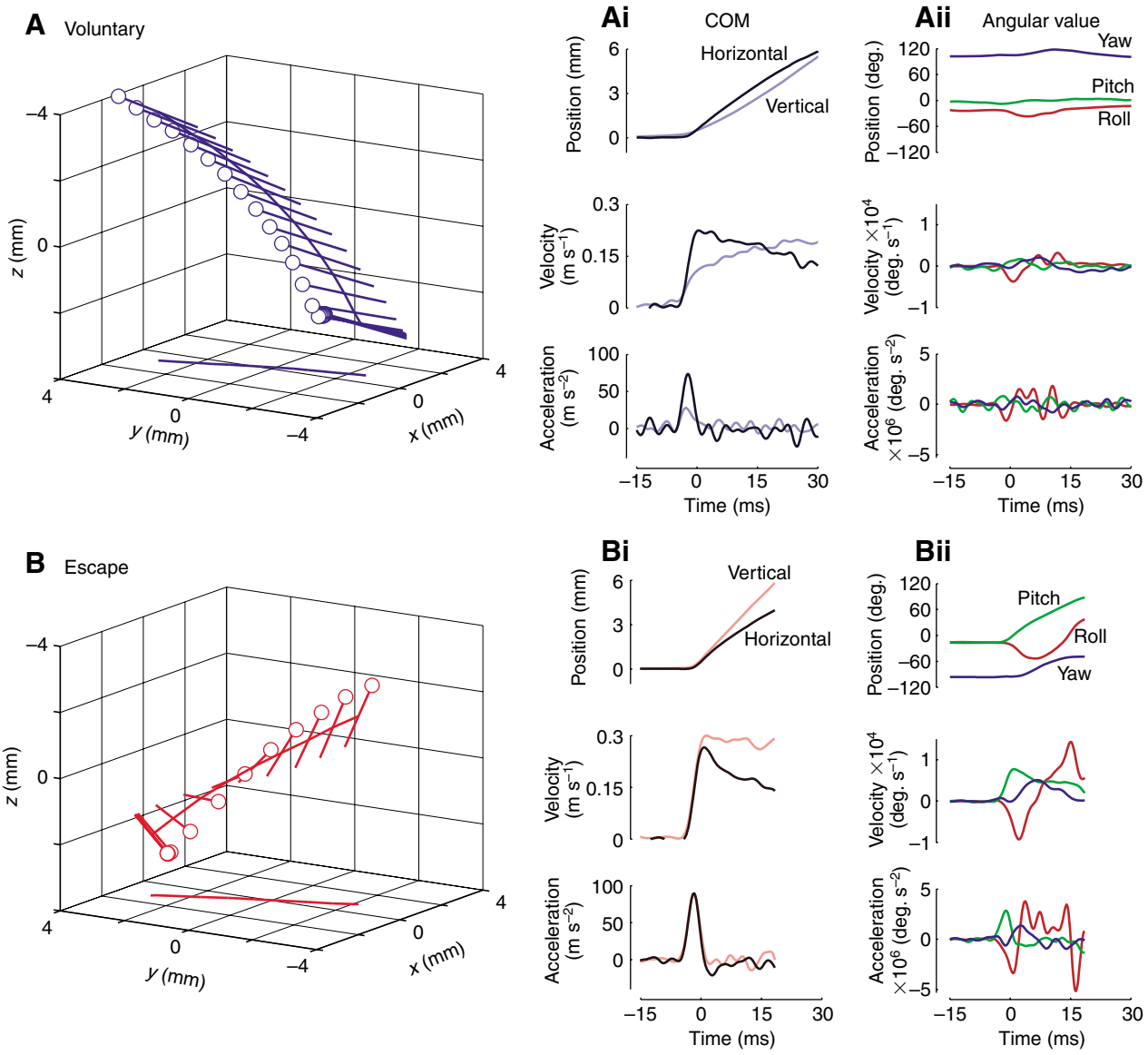

Fig. 6. Example body kinematics for an (A) voluntary and (B) escape take-off. Lollipop diagrams show the 3D position of the fly during take-off. Lines represent the long axis of the fly, and the open circle represents the position of the fly's head. Positions are plotted every 2.5 ms. The center of mass (COM; Ai, Bi) was defined as the point along the long body axis of the fly 45% of the distance from the head to the tip of the abdomen. We defined the starting COM location of the animal to be the origin. Horizontal position of the COM is the Euclidian distance traveled in the horizontal (*x*-*y*) plane (parallel to the ground) from the starting position. Angular values (Aii, Bii) are expressed in a body-centered frame of reference. Roll, pitch and yaw position are the cumulative rotations around the x_b, y_b, and z_b body axes, respectively (see Fig. 1 for axes definitions). The fly's starting position was determined by solving for the roll, pitch and yaw angles associated with the rotation required to move the body-centered frame from alignment with the lab frame to alignment with the fly's starting position.

twice as large for escapes compared to voluntary take-offs (e.g. pitch: 5710±661 deg. s^{-1} escape *vs* 2370±350 deg. s^{-1} voluntary), whereas peak roll velocity during escapes was more than three times that measured during voluntary take-offs and reached values greater than 10 000 deg. s^{-1} (10 200±1480 deg. s^{-1} escape *vs* 2860±1090 deg. s^{-1} voluntary). Further, instead of developing roll after take-off, as in the voluntary case, initial roll acceleration during escape occurred almost entirely during leg extension. Because escaping flies do not have their wings open during leg extension, the large roll acceleration must be produced primarily by the legs. Once airborne, escaping flies underwent a significant roll deceleration that returned the fly to a roll displacement of similar magnitude to that of flies performing voluntary take-offs by about 20 ms into the flight.

Speed *vs* control

The differences in escape and voluntary take-off performance can be characterized from the measured body kinematics by comparing their translational and rotational speeds. Translational speed relates to how quickly a fly is able to move away from an approaching threat, whereas rotational speed may indicate less stable flight, especially when it is composed of large roll and pitch components, as observed in escape flight (Fig. 7B). The speed of the fly along its flight path is simply the vector sum of the horizontal and vertical

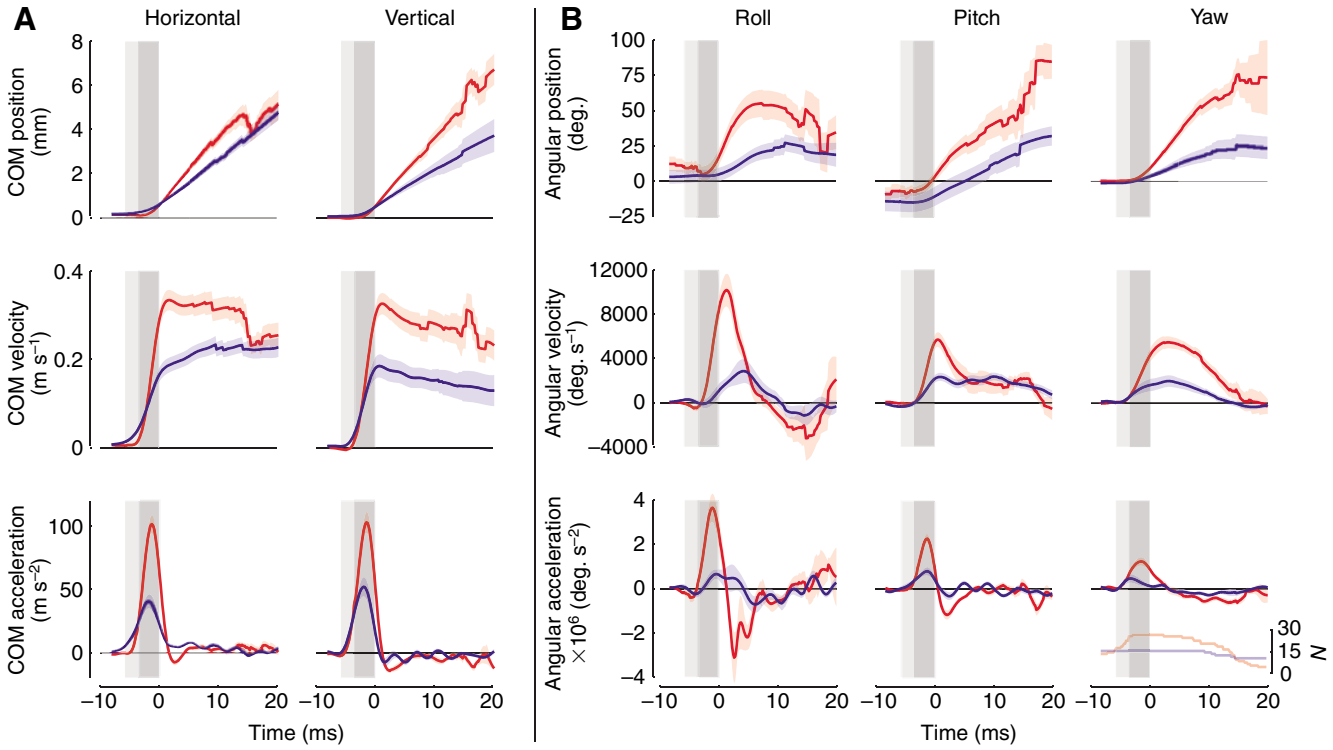

Fig. 7. Average time courses for (A) translational and (B) rotational kinematic variables. Blue lines are mean values for voluntary take-offs and red lines are mean values for escape responses. Shaded area around the mean shows the standard error. Time courses are aligned so that lift-off occurred at 0 ms. The yaw angular position was adjusted to start at 0°. Roll and pitch starting positions for each fly were defined as in Fig. 5. Roll and yaw values for position, velocity and acceleration have been adjusted as if all first rolling and yawing motions were to the fly's right. The dark grey region represents the median time of leg extension for escape take-offs, and the light and dark grey regions together indicate the median time of leg extension for voluntary take-offs. Individual flies did not remain in the field of view of our cameras for uniform amounts of time (see Figs 2 and 6). The inset in the lower right hand corner of B shows the number of flies averaged at each point in time. See also supplementary material Fig. S2 for alternate conventions describing take-off rotations.

center of mass velocity components. We define a relative steadiness metric S that is a linear transformation of the fly's angular speed:

$$S = 1 - ||\boldsymbol{\omega}|| / ||\boldsymbol{\omega}||_{\max} , \quad (6)$$

where $||\boldsymbol{\omega}||$ is the vector sum of the angular velocity about all three body axes, and $||\boldsymbol{\omega}||_{\max}$ is the largest angular speed observed in our experiments, 30 500 deg. s^{-1}. When S=1, the fly was maximally stable, with angular speed 0 deg. s^{-1}, and when S=0, the fly was maximally perturbed.

Fig. 8A shows the time courses of COM speed for both voluntary and escape take-offs. Escaping flies clearly accelerated more rapidly and achieved a higher initial velocity than those that took off voluntarily. Over the first 2 ms of flight, average COM speeds were 0.48±0.01 m s^{-1} and 0.28±0.02 m s^{-1} for escape and voluntary take-offs, respectively (P≪0.001, ANOVA). Escape speeds approached the maximum flight speeds observed in *Drosophila* (0.6 m s^{-1}) (David, 1979; Budick and Dickinson, 2006), whereas voluntary launch velocity was closer to the average cruising speed of the fly (0.35 m s^{-1}) (Budick and Dickinson, 2006). It is thus not surprising that, once in the air, flies that took off voluntarily were able to maintain a steady flight speed whereas those escaping slowed down over the first 5 ms of flight.

Fig. 8B shows the time courses of our steadiness metric S for voluntary and escape take-offs. For both conditions, angular speed peaked just after the fly left the ground, resulting in the lowest steadiness at this time. Flies taking off voluntarily, however, were more than 1.5 times as steady as escaping flies during the first 2 ms of flight (S=0.86±0.01 voluntary *vs* 0.55±0.03 escape; P≪0.001, ANOVA) and still had greater steadiness nearly 20 ms into the flight. From the video sequences, it is evident that the angular speed of escaping flies was the result of uncontrolled tumbling around all three body axes. Many of these tumbling flies pitched up past 90° (Fig. 2B), such that they were essentially flying upside-down.

A performance trade-off between speed and stability during take-off is clear from Fig. 8. Whereas average take-off velocity was greater for escapes compared to voluntary take-offs, escapes also produced significantly more rotational velocity, resulting in unsteady flight. Other evidence confirms the priority of speed over control in escape responses. Fig. 8A shows that escape flight speed declined for a short period immediately after take-off, but was still higher than the speed of voluntary jumpers after 10–20 ms in the air. Also, tarsal contacts tended to slip more during escape take-offs (38%) than during voluntary take-offs (19%), a difference that is most likely due to faster leg extension. Although take-offs in which the fly slipped were not analyzed, we observed from the video sequences that slipping during take-off usually led to extensive tumbling once airborne, as would be expected since uneven force between the two legs tends to induce the fly to roll.

Clipped wing flies

To measure the effects of body drag and assess the role of the wings during take-off, we clipped off the wings of eight flies and then elicited escape responses with the falling disk. Clipped-wing flies, not surprisingly, never exhibited a voluntary take-off. Remarkably,

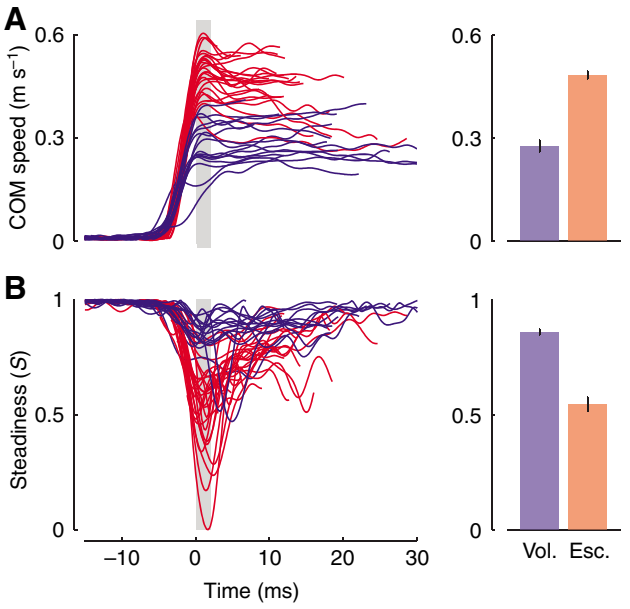

Fig. 8. Speed *vs* steadiness. (A) Time courses of center of mass (COM) speed shown for individual flies. Time courses are aligned so that lift-off occurred at 0 ms, and individual time courses end when the fly left the field of view of our cameras. The bar plot at the right indicates the COM speed (mean ± s.e.m.) for all flies over the first 2 ms of flight (grey region). (B) Time courses for steadiness (*S*) shown for individual flies. Steadiness was calculated from angular speed as described in the text, with large *S*-values corresponding to low angular speeds. Bar plots show steadiness (mean ± s.e.m.) over the first 2 ms of flight as in A. Voluntary (Vol.) trials are shown in blue, escape (Esc.) trials in red. Mean COM speed and steadiness are significantly different between voluntary and escape conditions, $P \ll 0.001$, ANOVA.

however, they did respond to the looming stimulus used in our experiments. All eight of the clipped-wing flies initiated 'flight' in response to the stimulus (Fig. 9A).

Time courses of kinematic parameters for all eight clipped-wing flies (means ± s.e.m.) are shown in Fig. 9C. Clipped-wing take-offs had a median leg extension time of 3.5 ms (IQR=0.8) similar to that of escape take-offs (NS, P=0.07, Kruskal–Wallis test), but significantly shorter than that of voluntary take-offs ($P \ll 0.001$, Kruskal–Wallis test). Note that, as expected from a simple ballistic model, the horizontal position of the fly's center of mass increased linearly while the vertical position described a roughly parabolic trajectory. Horizontal velocity was relatively constant once the fly was airborne, whereas vertical velocity declined linearly, becoming negative as the fly began to fall back towards the ground. The mean peak acceleration produced by the fly during leg extension was 46.9±10.4 m s^{-1} in the horizontal direction, and 58.2±10.1 m s^{-1} in the vertical direction, which is the same as that produced during voluntary take-offs (NS, P>0.9, ANOVA).

Clipped-wing take-offs differed most prominently from both voluntary and escape responses in the time course of angular velocity. For the first 2 ms in the air, clipped-wing flies had a mean steadiness value of 0.38±0.09 compared to 0.86±0.01 for voluntary or 0.55±0.03 for escape take-offs. Fig. 9D shows that the unsteady trajectory of clipped-wing flies was largely due to the extensive roll induced during the jump. Peak roll acceleration for the take-off of clipped-wing flies occurred during leg extension, as with intact flies, further confirming that in both cases the roll moment was created by the legs. In wingless flies, roll velocity remains roughly constant once airborne, indicating that air friction generated by the body was insufficient to decelerate the animal substantially. The continuous rotation about the roll axis was in sharp contrast to what we observed in intact escaping flies, which appear to produce counter roll once airborne. Such counter roll might be generated either passively *via* wing drag or actively *via* compensatory reflexes.

Because clipped-wing flies cannot produce force once in the air, we can assume that any observable acceleration is due to gravity or body drag. We quantified the effect of body drag after take-off by comparing the observed airborne COM velocity of each clipped-wing fly with the expected velocity if there was no effect of drag. In this frictionless model, the horizontal velocity of the airborne fly remains constant, and its vertical velocity declines at a constant rate of 9.8 m s^{-2} due to the effects of gravity. We found that the observed velocity of the clipped-wing flies deviated from the model with an average root mean square error (RMSE) of 0.04±0.005 m s^{-1}. We also calculated the RMSE for the best polynomial fit to the horizontal and vertical velocity components. The best fit for both components was a linear model, and the resulting average RMSE for the velocity magnitude was 0.03±0.004 m s^{-1}. The distributions of RMSE for the frictionless model and the best-fit polynomial model were not significantly different (P=0.12, ANOVA), indicating that the effects of body drag are smaller than the noise in our kinematic data. However, the noise in the kinematic data for the clipped-wing flies was larger than in the other experiments due to the lower frame rate (2000 frames s^{-1}) and lens magnification used to capture the entire jump of the flies. Also the clipped-wing flies rotated significantly more than the intact-wing flies, exacerbating any small errors in our estimation of the center of mass location. The average best-fit slope for the horizontal velocity component was –0.2±0.20 m s^{-2}, which was only slightly different from the slope of 0 m s^{-2} predicted by the frictionless model (P=0.02, one-sample t-test), and the average best-fit slope for the vertical velocity component was –10.2±0.27 m s^{-2}, which was only slightly larger in magnitude than the expected –9.8 m s^{-2} if only gravity, and not drag, were affecting the fly's trajectory (P=0.004, one-sample t-test). Based on this analysis, we conclude that the effects of drag are very small during take-off and thus the body dynamics of wingless flies are dominated by inertia.

DISCUSSION

Using high-speed videography we examined the flight performance of *Drosophila melanogaster* during two different kinds of flight initiation: escape responses elicited with a falling black disk and voluntary take-offs that were not deliberately stimulated (Fig. 2). Voluntary take-offs began with wing opening (rotation and elevation), followed, with quite a variable delay, by leg extension and simultaneous wing depression (Fig. 3). We observed that the wings were opened independently of each other, with the fly first raising whichever wing rests on top (Table 1). The largest time observed between the start of top and bottom wing opening was 140 ms, representing a substantial neural delay, given the rapidity of the subsequent phases of take-off behavior.

We were able to elicit escape take-offs reliably in red-eyed, wild-type flies using a falling black disk as stimulus. Under these conditions, we observed that take-offs, which were previously characterized by the absence of wing raising are, in fact, proceeded by variable degrees of wing elevation. This confirms the recent observations of Hammond and O'Shea, who used similar stimuli to elicit escape responses in *Drosophila* (Hammond and O'Shea,

2007a). In most escapes, however, we found that the fly did not fully raise its wings prior to the start of the jump, resulting in abnormal stroke kinematics during the first few cycles (Fig. 5). Instead, the wings were typically folded down against the body during leg extension and then, once airborne, bent ventrally at a joint distal to the wing hinge proper during the first few upstrokes. Although escape responses were somewhat variable, this peculiar pattern of wing motion during the first several stroke cycles was quite consistent.

We evaluated the two types of flight initiation and found that, although voluntary take-offs produced very steady flight with little rotation once airborne, they were relatively slow both with respect to the time required to get off the ground and the initial take-off velocity (Fig. 8). Escape take-offs, by contrast, occurred rapidly and accelerated the fly to a faster initial speed, but resulted in high rotational velocities after launch. Roll velocity was the largest contributor to the elevated angular velocity during the initial stages of an escape take-off and was quite distinct from the time course of roll during voluntary take-offs (Fig. 7B). Collectively, these results suggest a fundamental trade-off between take-off velocity and stability during flight initiation.

The role of wings

It seems paradoxical that voluntary take-offs had lower speeds than escapes, even though during the former flies used two types of appendages, wings and legs, to launch themselves into the air, while during the latter flies typically used only their legs. Since we observed that voluntary take-offs had greater steadiness (lower angular velocities) than escapes, we can rule out the possibility that this discrepancy in speed was the result of voluntary take-off forces not being directed through the fly's center of mass, producing more rotation and less forward speed. If anything, the greater steadiness of voluntary take-offs suggests that the launch forces are directed more precisely through the center of mass in the voluntary case. The two more likely explanations are that either (1) the fly's outstretched wings during voluntary take-off add a significant amount of drag, thereby slowing the fly during leg extension, or (2) the fly's legs do less work during voluntary take-offs than during escapes.

To evaluate the magnitude of drag effects, we removed both wings from a set of flies that performed escape jumps. These flies were unable to produce force once in the air, so changes in their airborne velocity must be attributable to deceleration from body drag and gravity. Our analysis found that the effects of drag on flight speed were so small as to be within the noise of our kinematic measurements. The launch velocity of voluntary take-offs, however, was 50% slower than that of escapes. Even if the effective area of the fly is tripled by the addition of outstretched wings – roughly tripling the effect of drag – drag alone cannot account for this lower velocity during voluntary take-off.

Another way of testing the role of flapping wings in decelerating the fly at the onset of flight is to make use of the variability of escape take-offs. If flapping wings substantially increase total drag compared to static wings, we would expect that in the subset of escape responses in which the flies successfully elevate both wings prior to the start of leg extension, the take-off velocity would be

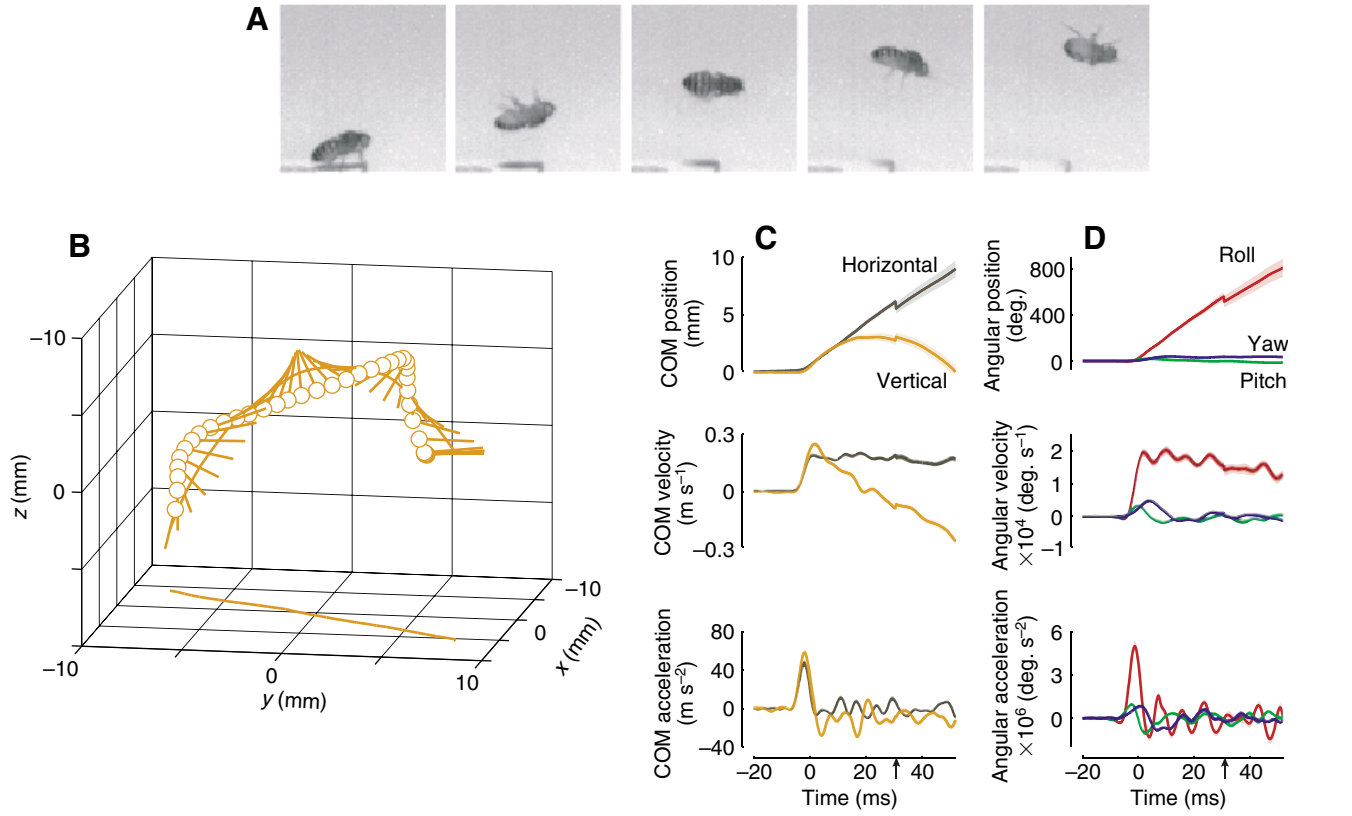

Fig. 9. Kinematics of escape responses for clipped-wing flies. (A) Video sequence of an example clipped-wing fly escape response to a falling disk stimulus. (B) Lollipop diagram of an example clipped-wing escape response showing the 3D position of the fly every 2.5 ms. (C,D) Average time courses (solid line, mean; shaded area, ± s.e.m.) for translational and rotational kinematic variables during clipped-wing take-off (as in Fig. 5). *N*=8 before the arrow on the time axis, and *N*=7 afterwards.

slower than cases in which the wings were held down against the body. To examine this hypothesis, we divided the escape responses into three categories based on the position and action of the wings during leg-extension: (1) take-offs in which both wings were elevated prior to leg extension and executed a downstroke similar to that during a voluntary take-off, (2) take-offs in which only one wing was completely elevated before leg-extension, or both wings reached only some intermediate opening position, and (3) take-offs in which the wings were raised only a small amount before being pulled down against the back of the fly. Fig. 10A shows the median take-off velocity for these three conditions as well as for voluntary take-offs and clipped-wing escapes. Escape responses in which the wings were successfully raised (‘**Esc’) had take-off velocities indistinguishable from escapes in which the wings were closed (‘Esc’), supporting the notion that increased wing drag cannot explain the lower initial velocities during voluntary take-offs. Furthermore, the take-off velocity of clipped-wing flies was even lower than that of intact flies during escapes. We conclude that the wings do not appear to make a significant contribution to total drag during the jump.

The role of legs

If drag forces cannot account for the higher speed of escapes compared to voluntary take-offs, could a difference in force production by the legs explain the discrepancy? If the legs are providing the only propulsive force during the majority of escape take-offs, and their extension is coordinated by a single spike in TTM, one would expect the legs to produce roughly the same amount of force during every escape. We observed, however, that escapes by clipped-wing flies were slower than those by intact flies (Fig. 10A). In this case, the large angular speeds of clipped-wing

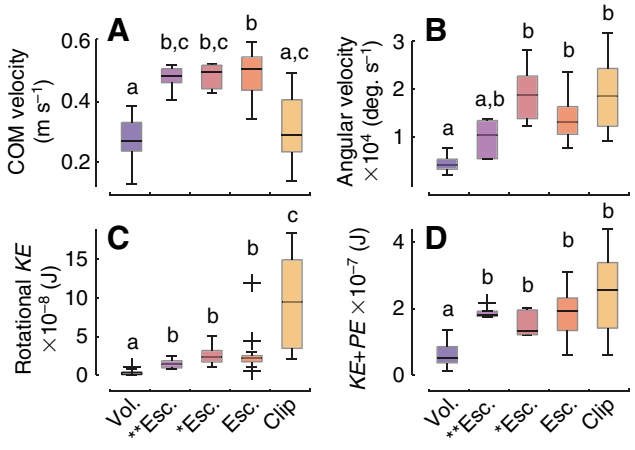

Fig. 10. Distributions of kinematic variables under different wing-raising conditions: voluntary take-off (Vol., *N*=16), escape take-offs with both wings raised before leg-extension (**Esc., *N*=5), escape take-offs with only one wing fully raised or wings only partially raised before leg-extension (*Esc., *N*=5), remaining escape take-offs in which wings move only minimally before leg-extension (Esc., *N*=17), and escape take-offs by flies with wings removed (Clip, *N*=8). Box plots are of values averaged over the first 2 ms of flight for (A) center of mass (COM) speed, (B) angular speed, (C) rotational kinetic energy, calculated from the angular speed and assuming the fly to be an ellipsoid body, and (D) the sum of potential (*PE*) and kinetic energy (*KE*). Kinetic energy is the sum of rotational kinetic energy (C) and translational kinetic energy (see text for derivation). Statistically significant differences were determined using Mann–Whitney pairwise comparisons with Bonferroni correction for multiple comparisons. Comparisons for which $P \leqslant 0.05$ are marked by different lower case letters.

fly take-offs (Fig. 10B) indicate that it is possible the legs are providing the same amount of work as in intact flies, but that the line of force acts further from the center of mass. The result would be that the airborne fly rotates more and translates forward less quickly. To determine whether this explanation is feasible, we estimated the amount of translational and rotational kinetic energy the fly generated during take-off, as well as the potential energy it had achieved during its first 2 ms in the air (see Materials and methods). The average total energy of the fly during the first 2 ms after take-off is the sum of translational, rotational and potential energies. From the airborne portion of our clipped-wing experiments, we know the effect of drag is minimal, so we neglect the effects of air resistance. Fig. 10C shows that the clipped-wing flies have significantly more rotational energy immediately after take-off than all intact-wing flies. The result of this rotation is that, although they have slower translational take-off velocities, clipped-wing flies actually have the same amount of total energy after take-off as other escaping flies (NS, $P>2$, Mann–Whitney pairwise comparison with Bonferroni correction, Fig. 10D), and that all escaping flies have greater total energy than voluntarily jumping flies ($P \ll 0.026$, Mann–Whitney pairwise comparison with Bonferroni correction). Thus, the legs of clipped-wing and intact-wing flies perform the same amount of work during take-off, but for clipped-wing flies a larger proportion goes into rotating the body rather than translating it. Such a difference might easily arise if, during take-off, the leg forces of clipped-wing flies act through a point that is farther from the center of mass than in the intact-wing case. Flies taking off voluntarily both translate and rotate more slowly, indicating that the legs perform much less work in this case.

If the work produced by the legs during an escape is the result of a single twitch in each jump muscle, how could these muscles produce less force during a voluntary take-off? One possibility is that the physiological state of the TTM muscle is different during the two behaviors. Octopamine has been suggested as a neuromodulator that can increase individual twitch strength in a jump muscle of locusts. In this system, octopamine is delivered by an octopaminergic midline neuron, DUM5A, at the correct time to enhance the contraction of the slow extensor tibia (SETi) muscle (Duch et al., 1999). Mutant *Drosophila* with defects either severely reducing the amount of octopamine available (Tbh^{nM18}) or lacking a strong octopamine receptor (TyR^{homo}) do not produce as much force with the mesothoracic legs when the GFs are stimulated and do not jump as far in assays where the wings are removed (Zumestein et al., 2004). This suggests that octopamine might enhance TTM force production during GF-mediated escapes but not during voluntary take-offs. However, it is still unclear whether the octopaminergic system in *Drosophila* could deliver the neuromodulator to the muscle within the tens of milliseconds timescale required to make it effective during escapes.

A second possibility is that all the extensor muscles of the leg, including the large TTM, are coordinated more effectively to generate greater power during escapes. This hypothesis is supported by the observation that the period of leg extension is shorter during escape take-offs. The GF is known to drive the tibial levator muscle (TLM), which extends the femur–tibia joint, with a characteristic latency of 0.6 ms after activation of the TTM (Trimarchi and Schneiderman, 1993). The TLM not only provides additional muscle force, but extension at the femur–tibia joint may help to keep the legs in contact with the substrate longer, prolonging the time during which leg muscle forces can act against the ground. The circuits underlying voluntary take-offs might coordinate TTM

and TLM muscles differently to push the fly off the ground more slowly but with less rotation.

Components of the flight initiation system

Based on our observations and those in the literature, we propose a simple scheme of descending command pathways to explain the differences between voluntary and escape take-offs in *Drosophila* (Fig. 11). Bilateral wing elevation pathways are required to explain how the fly can raise its left and right wings independently and with variable delay. In addition, the fly must possess two means of driving leg extension: the GFs and another, yet-to-be-identified, smaller diameter pathway. The existence of a second pathway is required by the evidence that flies can initiate take-off even when the GFs are not active (Holmqvist, 1994; Trimarchi and Schneiderman, 1995b).

As has been suggested (Hammond and O'Shea, 2007a), the fact that wing motion precedes the jumping phase of escape challenges the notion that the large-diameter GF interneurons trigger the first response to a threatening stimulus. GF stimulation is known to activate indirect wing elevators (dorsoventral muscles, DVMs) and a direct wing opener, pa3 (also known as b2) (see Wisser and Nachtigall, 1984), but with much longer latencies than the activation of the leg extensors (TTMs) and wing depressors (DLMs) (Tanouye and Wyman, 1980; Tanouye and King, 1983). Based on this well-characterized sequence of muscle activation, it is not possible for the GFs themselves to drive wing elevation prior to leg extension. One possible exception would be if the TTM muscle itself acts as a wing-opener, as has been suggested previously (Tanouye and King, 1983; Bacon and Strausfeld, 1986). If this is true, then some of the wing motion observed before the jump might be due to GF-driven TTM contraction. Even in this case, however, the GF pathway could not account for the cases in which the wings elevate several milliseconds or more before the onset of leg extension, a delay that is quite common during escapes (Fig. 3). Thus, the fact that the wings begin to open before the legs extend argues strongly for a small-diameter wing elevator pathway that is active before the GFs fire.

Although it seems unlikely that one or more spikes could travel more quickly along another axon than down the largest descending fibers in the neck connective, the initial activation of the GF system is temporally limited by the processing time within the visual system. A small-diameter descending interneuron that receives input from faster sensory modalities, such as the ocelli or antennae, might reach threshold much earlier, making up for its slower conduction speed and starting wing elevation before the GF spike arrives in the thorax. The descending interneurons of this putative pathway are likely to receive either local or ascending mechanosensory information because the circuit correctly raises the top wing first.

According to the scheme described in Fig. 11A, the functional performance of the take-off depends critically on the latency τ between wing activation and leg activation. Kinematic results indicate that steadiness S increases directly with increasing latency between the start of wing elevation and leg extension, for both voluntary and escape take-offs (Fig. 11A). Longer latencies presumably allow the fly to elevate its wings to a ready position before the start of the jump. Higher steadiness during take-off might be advantageous to a fly because it allows the fly to maintain its initial heading relative to an odor plume or wind direction, and minimizes the likelihood of an uncontrolled crash at the onset of flight. In the case of a threatening stimulus, however, a faster launch velocity may be of primary importance. In these cases, the GF-system elicits a powerful jump before the wing raising program has time to finish, resulting in a short wing-leg latency τ and a 'tuck and jump' take-off.

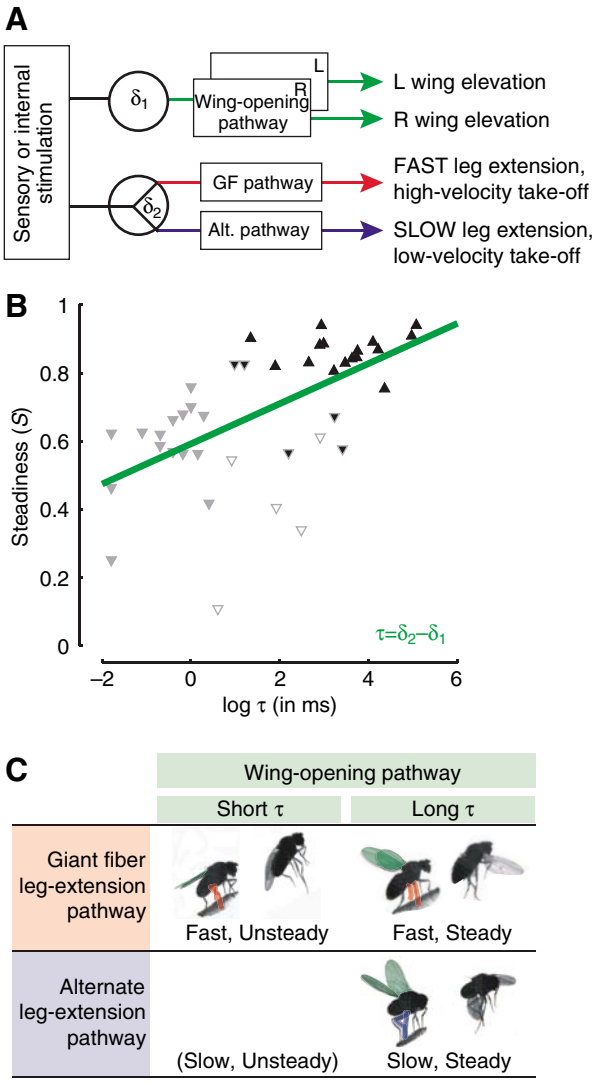

Fig. 11. Model for achieving take-off performance. (A) We hypothesize that a minimum of four independent pathways are required to coordinate take-off behavior: one coordinating wing opening on either side of the body and two coordinating different types of leg extension. In our model, take-off performance is determined by both the latency between activation of wing and leg pathways τ and the choice of leg pathway. In our diagram δ_1 represents the delay due to sensory and/or central processing before one or both wing pathways are activated, and δ_2 represents the delay before activation of one of the leg pathways. The difference between these two delay times is the observed wing–leg interval, τ. We propose that which leg pathway is activated for a given take-off determines the speed of that take-off. Alt., alternate. (B) The latency τ between wing and leg pathway activation determines take-off steadiness. This model is supported by our data: the graph shows the time τ between first wing motion and first leg motion plotted against the resulting take-off steadiness S for each fly observed (N=43). Upward-pointing triangles represent voluntary take-offs, while upside-down triangles mark escape responses. The fill color of the upside-down triangles (escapes) indicates the conditions of the wings during take-off, as defined in Fig. 10: black, **Esc. (N=5); white, *Esc. (N=5); gray, Esc. (N=17). The green line is a best-fit linear regression to the data. The line has a positive slope, indicating a direct correlation between τ and steadiness. (C) Summary of how coordination of the hypothesized pathways leads to the observed differences in take-off performance.

In addition, our data suggest that partially raised wings, or cases in which only one wing is fully raised, lead to lower steadiness at take-off than that predicted by their observed wing–leg latency (Fig. 11B, open triangles). This may explain why the giant fiber pathway activates the wing depressor muscles (DLMs) with such a short delay after the TTMs. Previous authors found the inclusion of the DLMs in the GF pathway paradoxical because they observed the wings to be closed before GF activation (Trimarchi and Schneiderman, 1995c). Hammond and O'Shea have revised this description, noting that the wings are typically elevated just before the escape jump (Hammond and O'Shea, 2007a). Our data further suggest that the functional role of pulling in the wings is not to lower translational drag (as might be assumed) but to reduce left–right wing differences, thus making take-off a bit more stable. An alternative view is that the added tumbling of the fly during escape may actually help the fly to avoid capture – in which case the early role of the DLMs in escape would require another explanation. In either case, modulating the latency between wing and leg pathway activation could be the mechanism by which the fly controls steadiness during take-off, trading it off against a faster reaction time when appropriate.

Another critical aspect of take-off performance is initial flight speed. Our data suggest that translational take-off velocity could be mediated by a choice between alternate leg-extension pathways. Body kinematics suggest that the mesothoracic legs produce more work during escape take-offs than during voluntary take-offs (Fig. 10D). If, as the literature suggests, escapes are mediated by the GF pathway and voluntary take-offs by an alternate pathway, then we hypothesize that use of the GF leg-extension pathway results in a strong, fast jump and a high take-off velocity. In contrast, use of the alternate leg-extension pathway results in a weaker, slower jump and a lower-velocity take-off (Fig. 10A).

Our hypothesized system is similar to the escape system found in the crayfish. The crayfish has two GF systems that coordinate stereotyped escape swimming either forward or backward, depending on the location of the stimulus. Both of these GF systems are activated by strong threatening visual or tactile stimuli. Milder stimuli, however, prompt a graded avoidance turn mediated by non-giant fiber pathways (Edwards et al., 1999). Together the GF systems and the non-giant pathways use the same musculature to create a range of responses to threatening stimuli, of which GF-mediated escape is at one extreme end. Our results indicate that *Drosophila* may be similarly equipped to employ a range of escape behaviors best tuned to type and magnitude of the threat (Fig. 10C).

LIST OF SYMBOLS AND ABBREVIATIONS

$\boldsymbol{g}$	acceleration due to gravity (9.8 m s^{-2})
COM	center of mass
DLM	dorsal longitudinal muscle
DVM	dorsal ventral muscle
GF	giant fiber
$\mathbf{I}$	moment of inertia tensor (kg m^2)
IQR	interquartile range
KE_{rot}	rotational kinetic energy
KE_{trans}	translational kinetic energy
m	mass (kg)
Med	median
PE	potential energy
PSI	peripherally synapsing interneuron
$\mathbf{q}$	quaternion
RMSE	root mean square error
S	steadiness
t	time
TLM	tibial levator muscle
TTM	tergotrochanteral muscle
v	translational velocity (m s^{-1})
z	height from ground (m)
τ	latency
$\boldsymbol{\omega}$	angular velocity vector (deg. s^{-1})

The authors wish to thank Will Dickson for his helpful discussion. This research was supported by grants from the National Science Foundation (0217229 and EF-0623527) and by a Gordon and Betty Moore fellowship.

REFERENCES

Abdel-Aziz, Y. I. and Karara, H. M. (1971). Direct linear transformation from comparator coordinates into object space coordinates in close-range photogrammetry. In *Proceedings of the ASP/UI Symposium on Close-Range Photogrammetry*, pp. 1-18. American Society of Photogrammetry.

Allen, M. J., Godenschwege, T. A., Tanouye, M. A. and Phelan, P. (2006). Making an escape: development and function of the *Drosophila* giant fibre system. *Semin. Cell Dev. Biol.* **17**, 31-41.

Bacon, J. P. and Strausfeld, N. J. (1986). The dipteran giant fiber pathway – neurons and signals. *J. Comp. Physiol. A* **158**, 529-548.

Budick, S. A. and Dickinson, M. H. (2006). Free-flight responses of *Drosophila melanogaster* to attractive odors. *J. Exp. Biol.* **209**, 3001-3017.

Card, G. M., Altshuler, D. and Dickinson, M. H. (2005). A directional escape response in *Drosophila melanogaster*. *Society for Neuroscience*, Program No. 176.14. Washington, DC.

David, C. T. (1979). Optomotor control of speed and height by free-flying *Drosophila*. *J. Exp. Biol.* **82**, 389-392.

Duch, C., Mentel, T. and Pfluger, H. J. (1999). Distribution and activation of different types of octopaminergic DUM neurons in the locust. *J. Comp. Neurol.* **403**, 119-134.

Edwards, D. H., Heitler, W. J. and Krasne, F. B. (1999). Fifty years of a command neuron: the neurobiology of escape behavior in the crayfish. *Trends Neurosci.* **22**, 153-161.

Fry, S. N., Sayaman, R. and Dickinson, M. H. (2003). The aerodynamics of free-flight maneuvers in *Drosophila*. *Science* **300**, 495-498.

Fry, S. N., Sayaman, R. and Dickinson, M. H. (2005). The aerodynamics of hovering flight in *Drosophila*. *J. Exp. Biol.* **208**, 2303-2318.

Hammond, S. and O'Shea, M. (2007a). Escape flight initiation in the fly. *J. Comp. Physiol. A* **193**, 471-476.

Hammond, S. and O'Shea, M. (2007b). Ontogeny of flight initiation in the fly *Drosophila melanogaster*: implications for the giant fibre system. *J. Comp. Physiol. A* **193**, 1125-1137.

Holmqvist, M. H. (1994). A visually elicited escape response in the fly that does not use the giant fiber pathway. *Vis. Neurosci.* **11**, 1149-1161.

Holmqvist, M. H. and Srinivasan, M. V. (1991). A visually evoked escape response of the housefly. *J. Comp. Physiol. A* **169**, 451-459.

Kaplan, W. D. and Trout, W. E. (1974). Genetic manipulation of an abnormal jump response in *Drosophila*. *Genetics* **77**, 721-739.

Kuipers, J. B. (2002). *Quaternions and Rotation Sequences: A Primer with Applications to Orbits, Aerospace, and Virtual Reality*. Princeton, NJ: Princeton University Press.

Levine, J. D. (1974). Giant neuron input in mutant and wild-type *Drosophila*. *J. Comp. Physiol. A* **93**, 265-285.

Lima, S. Q. and Miesenbock, G. (2005). Remote control of behavior through genetically targeted photostimulation of neurons. *Cell* **121**, 141-152.

Nachtigall, W. and Wilson, D. M. (1967). Neuro-muscular control of dipteran flight. *J. Exp. Biol.* **47**, 77-97.

Phillips, W. F. (2004). Aircraft flight simulation. In *Mechanics of Flight*, pp. 867-890. Hoboken, NJ: John Wiley & Sons.

Schilistra, C. and van Hateren, J. H. (1999). Blowfly flight and optic flow. I. Thorax kinematics and flight dynamics. *J. Exp. Biol.* **202**, 1481-1490.

Tanouye, M. A. and King, D. G. (1983). Giant fiber activation of direct flight muscles in *Drosophila*. *J. Exp. Biol.* **105**, 241-251.

Tanouye, M. A. and Wyman, R. J. (1980). Motor outputs of giant nerve-fiber in *Drosophila*. *J. Neurophysiol.* **44**, 405-421.

Thomas, J. B. and Wyman, R. J. (1984). Mutations altering synaptic connectivity between identified neurons in *Drosophila*. *J. Neurosci.* **4**, 530-538.

Tobalske, B. W., Altshuler, D. L. and Powers, D. R. (2004). Take-off mechanics in hummingbirds (*Trochilidae*). *J. Exp. Biol.* **207**, 1345-1352.

Trimarchi, J. R. and Schneiderman, A. M. (1993). Giant fiber activation of an intrinsic muscle in the mesothoracic leg of *Drosophila melanogaster*. *J. Exp. Biol.* **177**, 149-167.

Trimarchi, J. R. and Schneiderman, A. M. (1995a). Initiation of flight in the unrestrained fly, *Drosophila melanogaster*. *J. Zool.* **235**, 211-222.

Trimarchi, J. R. and Schneiderman, A. M. (1995b). Different neural pathways coordinate *Drosophila* flight initiations evoked by visual and olfactory stimuli. *J. Exp. Biol.* **198**, 1099-1104.

Trimarchi, J. R. and Schneiderman, A. M. (1995c). Flight initiations in *Drosophila melanogaster* are mediated by several distinct motor patterns. *J. Comp. Physiol. A* **176**, 355-364.

Wisser, A. and Nachtigall, W. (1984). Functional-morphological investigations on the flight muscles and their insertion points in the blowfly *Calliphora erythrocephala* (Insecta, Diptera). *Zoomorphology* **104**, 188-195.

Zumstein, N., Forman, O., Nongthomba, U., Sparrow, J. C. and Elliott, C. J. (2004). Distance and force production during jumping in wild-type and mutant *Drosophila melanogaster*. *J. Exp. Biol.* **207**, 3515-3522.